JOURNAL OF AGRICULTURAL AND FOOD CHEMISTRY
ARTICLE

J. Agric. Food Chem. 2010, 58, 8111–8118 8111
DOI:10.1021/jf100778f

Metabolites of Galangin by 2,3,7,8-Tetrachlorodibenzo-*p*-dioxin-Inducible Cytochrome P450 1A1 in Human Intestinal Epithelial Caco-2 Cells and Their Antagonistic Activity toward Aryl Hydrocarbon Receptor

Mika Hamada,*,† Hideo Satsu,† Hitoshi Ashida,‡ Yoshiko Sugita-Konishi,§ and Makoto Shimizu†

†Department of Applied Biological Chemistry, Graduate School of Agricultural and Life Sciences, The University of Tokyo, 1-1-1 Yayoi, Bunkyo-ku, Tokyo 113-8657, Japan, ‡Department of Agrobioscience, Applied Chemistry in Bioscience Division, Graduate School of Agricultural Sciences, Kobe University, 1-1 Rokkodai-cho, Nada-ku, Kobe 657-8501, Japan, and §Division of Microbiology, National Institute of Health Sciences, 1-18-1 Kamiyoga, Setagaya-ku, Tokyo 158-8501, Japan

Galangin, a dietary flavonoid, inhibited cytochrome P450 1A1 (CYP1A1) expression induced by 2,3,7,8-tetrachlorodibenzo-*p*-dioxin (TCDD). This inhibitory activity remained after permeating human intestinal epithelial Caco-2 cell monolayers, but was reduced when galangin permeated TCDD-pretreated Caco-2 cells. The present study tested whether TCDD affected the intestinal metabolism of flavonoids. LC-MS/MS analyses showed that galangin and two galangin glucuronoconjugates were reduced 0.7-fold, whereas kaempferol (a galangin oxidate) and kaempferol glucuronoconjugate were increased 1.5-fold by permeating TCDD-pretreated Caco-2 cells, as compared to untreated Caco-2 cells. An assay using recombinant human CYP1A1 and the CYP1A1 inhibitor α-naphthoflavone revealed that CYP1A1 oxidized galangin to kaempferol. These results indicated that galangin was metabolized to kaempferol by TCDD-inducible CYP1A1 in Caco-2 cells. A previous study revealed that kaempferol had much weaker inhibitory activity than galangin toward TCDD-induced CYP1A1 expression. Therefore, the oxidative metabolism of galangin to kaempferol in TCDD-pretreated Caco-2 cells implicated reduction in the inhibitory activity of galangin.

KEYWORDS: Caco-2; CYP1A1; galangin; keampferol; metabolism; TCDD

INTRODUCTION

Polycyclic aromatic hydrocarbons (PAHs) such as dioxins, exemplified by 2,3,7,8-tetrachlorodibenzo-*p*-dioxin (TCDD), are released as industrial compounds or byproducts through combustion. They cause serious problems as environmental contaminants. Various studies have been performed to elucidate the mechanisms underlying the toxic effects of dioxins. Whereas an aryl hydrocarbon receptor (AhR)-linked change in the gene expression of several xenobiotic-metabolizing enzymes, as typified by cytochrome P450 1A1 (CYP1A1), is widely accepted (*1*), genes exhibiting alteration and playing a major role in this toxicity remain largely unknown.

Although most dioxins are orally absorbed through contaminated food (*2*, *3*), removing dioxins from food is difficult and expensive. Therefore, searching for a food factor that prevents dioxin toxicity is important. Flavonoids in many types of vegetables and fruits are good dietary candidates for suppressing AhR transformation because they have a suitable structure for binding to AhR ligand-binding pockets (*4*). We previously studied the effect of flavonoids on the toxicity of TCDD using the following two in vitro evaluation methods: measuring AhR transformation by a southwestern chemistry-based enzyme-linked immunosorbent assay (SW-ELISA) and transcriptional activity of the CYP1A1 promoter by a luciferase assay (*5*). Absorption of flavonoids through the intestinal epithelium was also considered by introducing a human intestinal epithelial Caco-2 cell model into the evaluation system. This study demonstrated that seven flavonoids had a marked suppressive effect on dioxin toxicity; they were also effective after permeating the human intestinal epithelial Caco-2 monolayer. In particular, galangin, flavone, and tangeretin showed marked suppressive effect on the TCDD-induced increase in CYP1A1/CYP1A2 mRNA and CYP1A1 protein, although the quantity of these flavonoids and the structures of their metabolites after permeating the Caco-2 cell monolayer remain to be elucidated.

Flavonoids are absorbed and metabolized in the intestine. The potential activity of flavonoids in vivo is also dependent on intestinal absorption, this being followed by metabolic reactions and subsequent interaction with target tissues. Therefore, it is important to investigate metabolite structures and biological functions. Intestinal absorption, metabolism, and the distribution and excretion of flavonoids have been extensively studied. Eleven types of cytochrome P450 and 37 types of phase II

*Corresponding author (telephone +81 3 5841 5131; fax +81 3 5841 8026; e-mail mikage417@hotmail.co.jp).

Published on Web 06/15/2010

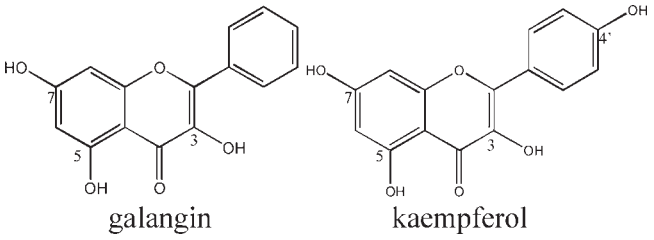

Figure 1. Chemical structures of galangin and kaempferol.

xenobiotic-metabolizing enzymes were expressed in Caco-2 cells after culturing for 16 days (*6*). These enzymes were involved in the intestinal metabolism of flavonoids; for example, chrysin and apigenin (a class of flavones) were mainly catalyzed by a conjugation pathway in Caco-2 cells, with both sulfated and glucuronidated forms being produced (*7*).

As mentioned, food is a major source of dioxin intake. The intestinal tract is exposed to a higher concentration of dioxin than any other organ. TCDD has been reported to induce xenobiotic-metabolizing enzymes such as CYP1A1 (*8*), UDP-glucuronosyltransferase (UGT) 1A6, and UGT 1A9 (*9*) in Caco-2 cells. Therefore, dioxins are considered to influence the metabolism of dietary flavonoids in intestinal epithelial cells and eventually alter the bioavailability of flavonoids.

The aim of the present study was to test whether TCDD affects the intestinal metabolism of flavonoids and whether their inhibitory activity toward TCDD toxicity changes after passing across intestinal cells. Using reporter analyses, we examined the suppressive effect of flavonoids, which permeated the TCDD-pretreated human intestinal Caco-2 cell monolayers, on inducible CYP1A1 transcriptional activity. Using LC-MS/MS, the quantity and structure of metabolites produced by Caco-2 cells, particularly galangin, were analyzed (**Figure 1**). The enzyme involved in the oxidative metabolism of galangin was also identified.

MATERIALS AND METHODS

Materials. The Caco-2 cell line (derived from human colonic cancer tissue) and HepG2 cell line (derived from human hepatic cancer tissue) were obtained from the American Type Culture Collection (Rockville, MD). Dulbecco's modified Eagle's medium (DMEM), apigenin, and α-naphthoflavone (ANF) were purchased from Sigma-Aldrich (St. Louis, MO). Penicillin−streptomycin (10000 U/mL and 10 mg/mL in 0.9% sodium chloride, respectively) and nonessential amino acids were purchased from Gibco (Gaithersburg, MD). Fetal bovine serum was purchased from Asahi Technoglass (Chiba, Japan). Twelve-well Transwell inserts and 24-well plates were purchased from Corning-Coster (Corning, NY). G418 disulfate was purchased from Nacalai Tesque (Kyoto, Japan), and TCDD and flavanone were purchased from Wako Pure Chemical Industries (Osaka, Japan). Galangin, kaempferol, and luteolin were obtained from Extrasynthese (Genay, France), and flavonol was obtained from Tokyo Kasei Kogyo (Tokyo, Japan). All other chemicals were of reagent grade.

Cell Culture. Caco-2 cells were cultured at 37 °C in a humidified 5% CO_2 atmosphere in a culture medium consisting of DMEM, 10% fetal bovine serum, 1% nonessential amino acids, 200 U/mL of penicillin, and 200 μg/mL of streptomycin. TCDD-responsive HepG2 cells stably transfected with the dioxin-responsive plasmid (pLUC1A1) were established as described previously (*10*). Nonessential amino acids were excluded from the culture of these stably transfected HepG2 cells (HepG2-LUC), and G418 was added to the same medium used for culturing Caco-2 cells. The Caco-2 cells were between passages 40 and 65.

Transepithelial Transport Experiments. To form Caco-2 cell monolayers, cells were seeded at 2×10^5 cells/well in a 12-well Transwell insert precoated with collagen and cultured for 2 weeks to obtain an integrated cell monolayer with a transepithelial electrical resistance of >150 ohm·cm^2. Each flavonoid sample was dissolved in dimethyl sulfoxide (DMSO) and added to the apical chamber (0.5 mL) of the Caco-2 cell monolayer to give a final flavonoid concentration of 10−100 μM. The apical and basal solutions (1.5 mL) were recovered after incubation and were analyzed by luciferase assay or LC-MS/MS.

Luciferase Assay. A luciferase assay was performed to examine whether the flavonoids could inhibit the TCDD-induced transcriptional activity of CYP1A1 in TCDD-responsive HepG2-LUC cells. HepG2-LUC cells were seeded at 5×10^4 cells/well in a 24-well plate precoated with collagen and used after 1 day of culture. Sample solutions containing a flavonoid together with TCDD (an AhR activator) were added to each well of the 24-well plate in which the HepG2-LUC cells had been seeded. The luciferase assay was performed after 24 h of incubation according to the instruction manual for the Dual-Luciferase reporter assay (Promega). The 24-well plate was washed twice with PBS, and the contents were dissolved in a 50 μL passive lysis buffer and used for the luciferase assay.

Western Blot Analysis. After incubation with galangin or TCDD, Caco-2 cells cultured in 6-well plates for 1 day were washed twice with ice-cold PBS. Cells were scraped off and then suspended in 1 mL of PBS. The precipitate obtained by centrifugation at 1000*g* for 5 min at 4 °C was homogenized with 0.1 mL of 0.1% SDS buffer (0.1% SDS, 50 mM Tris-HCl, 1 mM EDTA, 150 mM NaCl, 0.25% sodium deoxycholate, 0.1 mM phenylmethanesulfonyl fluoride, and 0.1% of an inhibitor cocktail) and left on ice for 20 min. The homogenate was centrifuged at 20000*g* for 15 min at 4 °C. The resulting supernatant was dissolved in a loading buffer containing 0.125 M Tris-HCl (pH 6.8), 14% glycerol, 4% SDS, 0.05% bromophenol blue, and 10% β-mercaptoethenol at 100 °C for 5 min.

Samples containing 30 μg of protein were loaded onto 12.5% polyacrylamide gel. Electrophoresis was conducted in an electrode buffer [25 mM Tris, 192 mM glycine, and 0.1% (w/v) SDS] with a fixed current (20 mA). An Immobilon polyvinylidene difluoride (PVDF) membrane (Millipore, Bedford, MA) was treated with methanol and then blotting buffer (100 mM Tris, 192 mM glycine, and 20% methanol). The Bio Craft semidry type of blotting apparatus was used for electrophoretic transfer of the gel to the PVDF membrane at 120 mA over 90 min.

After blotting, this PVDF membrane was blocked overnight at 4 °C by 0.1% Tween-20 and 5% skimmed milk dissolved in PBS. It was then incubated for 2 h with anti-human CYP1A1 antibody (1:100 dilution; sc-25304 Santa Cruz Biotechnology, Santa Cruz, CA), anti-human UGT1A antibody (1:500 dilution; sc-25847 Santa Cruz Biotechnology), or monoclonal anti-GAPDH antibody (1:2500 dilution; ab8245, Abcam, Cambridge, U.K.) dissolved in a Can Get Signal immunoreaction enhancer solution (Toyobo, Japan). After the PVDF membrane had been washed three times with 0.1% Tween-20 dissolved in PBS for 10 min each, it was incubated for 1 h with anti-mouse immunoglobulin G−horseradish peroxidase (IgG−HRP; 1:2000 dilution; NA931, Amersham Biosciences, Buckinghamshire, U.K.), anti-rabbit IgG−HRP (1:2500 dilution; NA934, Amersham Biosciences), or anti-mouse IgG−HRP (1:2000 dilution). Proteins were detected by an ECL Plus Western blotting detection system (Amersham Biosciences), followed by analysis with an LAS-4000 mini image analyzer and Multi Gauge Ver3.0 (Fuji Photo Film Co., Ltd., Tokyo, Japan).

Galangin Metabolism by Recombinant Human CYP1A1. Human CYP1A1 enzymes and control microsomes produced using a baculovirus−insect cell expression system and NADPH regenerating system solution were purchased from BD Gentest Co. (Woburn, MA). Galangin (10 μM) was incubated with recombinant human CYP1A1 (50 μg of protein) in 0.1 mL of potassium phosphate buffer (100 mM, pH 7.4) containing 5 μL of NADPH regenerating system solution A (1.3 mM $NADP^+$, 3.3 mM $MgCl_2$, and 3.3 mM G6P) and 1 μL of NADPH regenerating system solution B (0.4 U/mL of G6P dehydrogenase) at 37 °C. The reaction was stopped by adding an equivalent amount of acetonitrile. The concentrations of galangin and kaempferol in the incubated mixtures were measured by LC-MS/MS.

Sample Preparation for LC-MS/MS. Incubated galangin samples were added to an equivalent amount of acetonitrile and vortexed. After the sample had been centrifuged at 20000*g* for 5 min, the resulting supernatant was filtered with a 4 mm, 0.2 μm sterile syringe filter (Corning Costar). Five microliters of the resulting filtrate was injected into the LC-MS/MS system.

LC-MS/MS Analysis. Galangin and the metabolites were identified and quantified by LC-MS/MS analyses. LC analysis was performed with an 1100 series instrument (Agilent Technologies, Palo Alto, CA) equipped

with a quaternary pump and refrigerated autosampler. An Atlantis dC18 column (2.1 × 150 mm i.d., 3 μm) from Waters (Milford, MA) was used at 40 °C. Gradient elution was performed with water (0.1% acetic acid) and acetonitrile (0.1% acetic acid) at a constant flow rate of 0.2 mL/min. A gradient profile with the following proportions (v/v) of acetonitrile (0.1% acetic acid) was applied [time (min), % acetonitrile]: 0, 20; 1, 20; 41, 100; 51, 100; 52, 20; and 60, 20. An API 3000 triple-quadrupole mass spectrometer (Applied Biosystems, Concord, ON, Canada) equipped with a TurboIonSpray source was operated in the negative ion mode to obtain MS and MS/MS data. The ion spray flow was set at 6500 cm^3/min. Standard solutions of galangin and kaempferol were applied to optimize detection conditions in the LC mobile phase. Optimized parameters of ionization for the ion source (NEB, CUR, CAD, IS, and TEM) and for the analyzer (DP, EP, FP, CE, and CXP) are shown in **Table 1**.

A Q3MS (Q3) scan was employed to perform a full scan with an m/z range of 200−700 to capture all of the ions produced from the control (standard galangin) and sample (galangin incubated in Caco-2 cells). Information data acquisition and product ion (MS2) scans were subsequently used for in-depth investigation of the specific ions of interest, based on a Q3 comparison of the control and sample to obtain their fragmentation patterns. The corresponding MS2 spectra of potential metabolites were compared to that of galangin to investigate fragmentation patterns and obtain information on metabolite structures. A multiple reaction monitoring (MRM) mode analysis (the method of choice because of its high selectivity and sensitivity in quantitative LC-MS/MS analysis) was performed to quantify galangin and the metabolites. The precursor/product ion pairs for galangin and kaempferol were m/z 269.0/169.2 and m/z 285.0/185.4, respectively. Q1 and Q3 values were based on the biotransformation prediction of flavonoids by Metabolite ID 1.3 software (Applied Biosystems/MDS Sciex). The HPLC system and mass spectrometer were controlled by Analyst 1.4.2 software (Applied Biosystems/MDS Sciex).

Table 1. Mass Spectrometric Parameters

parameter	value: galangin (m/z 269.1/169.0)	value: kaempferol (m/z 284.9/185.0)
nebulizer gas (NEB)	12	
curtain gas (CUR)	10	
collision gas (CAD)	7	
ion spray voltage (IS)	−4000	
temperature (TEM)	300	
declustering potential (DP)	−86	
entrance potential (EP)	−10	
focusing potential (FP)	−210	−160
collision energy (CE)	−40	−38
collision cell exit potential (CXP)	−13	−15

Statistical Analysis. The data were expressed as the mean ± standard error (SE). Significance was determined by the t test or Tukey's multiple-comparison test. Differences were considered to be significant at $p < 0.05$.

RESULTS

Inhibitory Effect of Flavonoids That Permeated TCDD-Pretreated Caco-2 Cell Monolayers on Inducible CYP1A1 Expression. In our previous study, some flavonoids (apigenin, luteolin, flavanone, flavonol, and galangin) were found to have a markedly suppressive effect on the increased expression of CYP1A1 (*5*); these were also effective after permeating the human intestinal epithelial Caco-2 monolayer. In the present study, to determine whether TCDD affected the absorption and metabolism of flavonoids in intestinal cells, the inhibitory effect on the transcriptional activity of CYP1A1 was examined with flavonoids that permeated the Caco-2 cell monolayer pretreated with TCDD. A luciferase assay using dioxin-responsive HepG2-LUC cells (*10*) was performed to measure transcriptional activity. Each of the five previously reported flavonoids (apigenin, luteolin, flavanone, flavonol, and galangin) was added to the apical side of a Caco-2 cell monolayer pretreated with 2.5 nM TCDD for 24 h. After incubation, the basal media of the Caco-2 cell monolayers together with TCDD (2 nM) were added to a 24-well plate in which HepG2-LUC cells had been seeded, and the luciferase assay was performed 24 h later. TCDD elevated luciferase activity to 24-fold of the DMSO control (data not shown). All flavonoids (0−100 μM) that permeated the Caco-2 cell monolayers suppressed the inducible transcriptional activity of CYP1A1 in a dose-dependent manner (**Figure 2**). However, the effects of flavonoids that permeated the TCDD-pretreated Caco-2 cell monolayer were weaker than those that had permeated the untreated monolayers. Galangin, which had permeated the

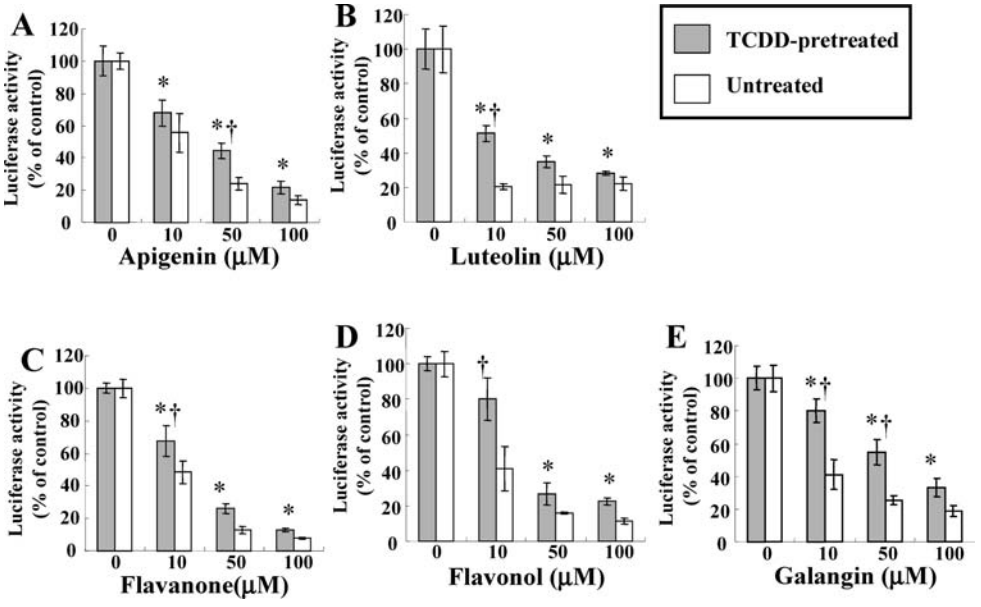

Figure 2. Effect of flavonoids that permeated TCDD-pretreated Caco-2 cell monolayers on CYP1A1 transcriptional activity. A flavonoid that permeated TCDD-pretreated Caco-2 cell monolayers and TCDD were added to HepG2-LUC cells, and a luciferase assay was performed 24 h later: **A**, apigenin; **B**, luteolin; **C**, flavanone; **D**, flavonol; **E**, galangin. The control (no added flavonoid) shows the results with only 2 nM TCDD. Each value is the mean ± SE ($n = 3$). *, $p < 0.01$, significantly different from the control; †, $p < 0.05$, significantly different from the untreated group analyzed by Tukey's multiple-comparison test.

TCDD-pretreated Caco-2 cell monolayer, had a significantly lower inhibitory effect on the transcriptional activity of CYP1A1 (**Figure 2E**, 10−50 μM). We therefore chose galangin, a dietary flavonol commonly present in medicinal plants, for subsequent experiments.

Amount of Galangin in Apical and Basal Chambers after Incubation with Caco-2 Cells. Galangin was added to the apical side of TCDD-pretreated or untreated Caco-2 cell monolayers. After incubation for 24 h, galangin in the medium of Caco-2 cells was quantified in the MRM mode. In the Transwell, about 17% of galangin that was added to the apical solution was transported to the basal chamber after 24 h of incubation (**Figure 3A**). This transport was decreased to 12% by pretreating Caco-2 cells with TCDD. Caco-2 cell monolayers in the 24-well plates were then used to further elucidate the decrease of galangin through the metabolic reactions in Caco-2 cells. After 24 h of incubation, about 18% of galangin remained in the medium of Caco-2 cells in the 24-well plates (**Figure 3B**). In the case of pretreatment with TCDD, only 10% of galangin added to the apical solution was detected. These results suggest that TCDD pretreatment activated the metabolism of galangin in the Caco-2 cells.

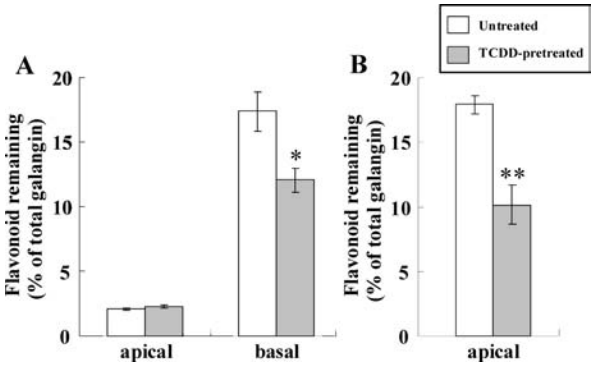

Figure 3. Amount of residual galangin after incubation with TCDD-pretreated or untreated Caco-2 cells. TCDD-pretreated or untreated Caco-2 cell monolayers in the Transwell insert (**A**) or 24-well plate (**B**) were incubated with 10 μM galangin for 24 h. Galangin was detected by LC-MS/MS. Data are expressed as a percentage of the total amount of galangin and presented as the mean ± SE (n = 3). ∗, $p < 0.05$, and ∗∗, $p < 0.01$, significantly different from the values for the untreated group analyzed by the t test.

Galangin Metabolites in Caco-2 Cell Monolayers and Their Quantitative Changes by TCDD Pretreatment. Galangin metabolites were analyzed by the same LC-MS/MS system with Metabolite ID for their identification. Comparison of the Q3 profiles for the control (standard galangin) and sample (galangin incubated in Caco-2 cells) showed four potential metabolites present only in the sample that had been eluted with a shorter retention time (t_R) than that of galangin. The potential metabolite with a t_R of 12.7 min and a MRM transition of m/z 285.0/185.4 was identified as the galangin oxidate kaempferol. The other three potential metabolites with t_R values of 10.2, 10.9, and 11.7 min were identified as the kaempferol glucuronoconjugate and two galangin glucuronoconjugates, respectively (**Figure 4** and **Table 2**). These metabolites were detected in the MRM mode, and the peak area ratio of each metabolite was calculated by dividing the peak area of the pretreatment with TCDD by that of no treatment. The amounts of kaempferol and its glucuronoconjugate produced by TCDD-pretreated Caco-2 cells were 1.57 and 1.53 times, respectively, more than those produced by the untreated cells in a 24-well plate. On the other hand, the galangin glucuronoconjugates were decreased 0.67-fold (t_R of 10.9 min)

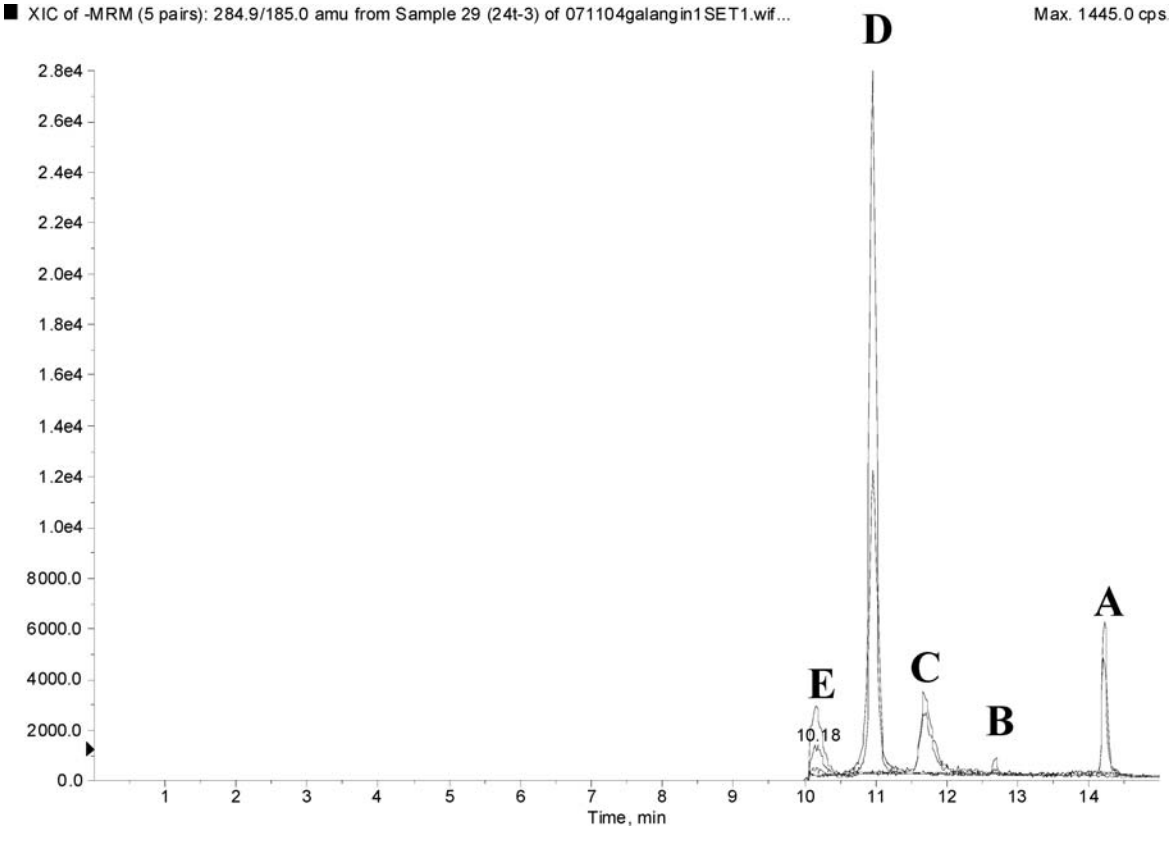

Figure 4. LC-MS/MS MRM chromatograms of galangin and metabolites. Peaks: A, galangin (m/z 269.1/169.0); B, kaempferol (m/z 284.9/185.0); C, galangin glucuronide (t_R of 11.7, m/z 269.1/169.0); D, galangin glucuronide (t_R of 10.9, m/z 269.1/169.0); E, kaempferol glucuronide (m/z 284.9/185.0).

Table 2. LC-MS/MS Retention Times, Mass Spectral Properties, and Peak Area Changes for Galangin Metabolites[a]

				peak area ratio (pretreated with TCDD/untreated)		
				Transwell		24-well plate
	t_R	MW	*m/z* of MS/MS ions	apical	basal	apical
galangin	14.0	270	169, 195, 223	1.10 ± 0.04	0.69 ± 0.05*	0.57 ± 0.09**
kaempferol glucuronide	10.2	462	285, 185			1.57 ± 0.01***
galangin glucuronide	10.9	446	269, 241	0.83 ± 0.02	0.86 ± 0.04*	0.67 ± 0.03**
galangin glucuronide	11.7	446	269, 113, 99	0.77 ± 0.02**		0.58 ± 0.02**
kaempferol	12.7	286	185, 155, 213	1.25 ± 0.04**	1.15 ± 0.09	1.53 ± 0.26

[a] The peak area ratio of each metabolite was calculated by dividing the peak area of the TCDD-pretreated Caco-2 cell sample by that of the untreated Caco-2 cell sample. Data are presented as the mean ± SE (n = 3). *, $p < 0.05$; **, $p < 0.01$; and ***, $p < 0.001$ are significantly different from the values for the untreated group analyzed by the t test.

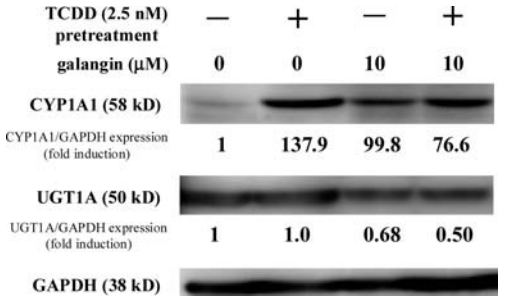

Figure 5. Effects of TCDD pretreatment and galangin on the expression of CYP1A1 and UGT1A proteins in Caco-2 cells. TCDD-pretreated or untreated Caco-2 cells were incubated with 10 μM galangin for 24 h, and the proteins in these cells were analyzed by Western blotting. Relative protein expression (control is set as 1) normalized to GAPDH represents two independent experiments.

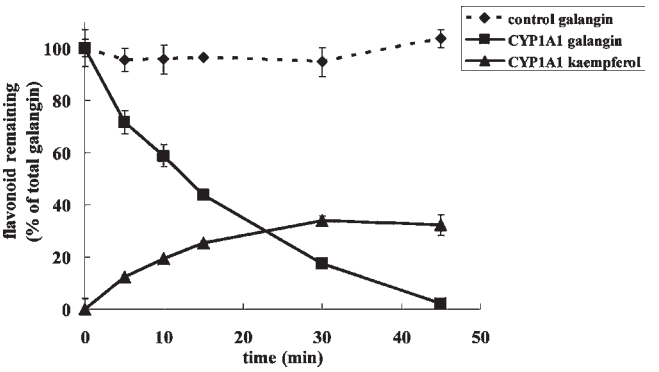

Figure 6. Time course characteristics for oxidation of galangin to kaempferol by recombinant human CYP1A1. Galangin and kaempferol concentrations were measured by LC-MS/MS and expressed as a percentage of the total amount of galangin used. Mean ± SE values (n = 3) are shown.

and 0.58-fold (t_R of 11.7 min) by pretreating Caco-2 cells with TCDD. These results suggested that TCDD pretreatment activated the oxidation of galangin to kaempferol in Caco-2 cells.

Effect of TCDD Pretreatment on Protein Expression of Xenobiotic-Metabolizing Enzymes. Galangin (10 μM) was added to Caco-2 cell monolayers pretreated with 2.5 nM TCDD, and CYP1A1 and UGT1A protein levels were analyzed by Western blot analysis. CYP1A1 was dramatically induced to 137.9-fold of control by TCDD pretreatment (**Figure 5**). Galangin markedly suppressed this TCDD-induced increase in CYP1A1 expression (76.6-fold of control), although galangin itself significantly induced CYP1A1 expression (99.8-fold of control). TCDD pretreatment for 24 h had no effect on UGT1A, whereas UGT1A expression decreased in cells treated with galangin compared to the control value.

Involvement of CYP1A1 in Oxidation of Galangin to Kaempferol. Recombinant human CYP1A1 was used to determine whether CYP1A1 was involved in the oxidation of galangin to kaempferol. CYP1A1 catalyzed the oxidation of galangin to kaempferol, as evident from the disappearance of galangin and the appearance of kaempferol during a 45 min incubation period (**Figure 6**). Although an appreciable amount of galangin was metabolized by CYP1A1, kaempferol formation was low. Other metabolites could not be detected by Metabolite ID analysis.

Inhibition of CYP1A1-Catalyzed Oxidation of Galangin to Kaempferol by ANF in Caco-2 Cells. Galangin and the CYP1A1 inhibitor ANF were added to Caco-2 cell monolayers to confirm that galangin was oxidized by CYP1A1 in Caco-2 cells. Because ANF has an agonistic and antagonistic effect on AhR (*11*), we confirmed that 1 or 10 μM ANF had no effect on CYP1A1 expression in Caco-2 cells during 3 h of incubation (**Figure 7B**). Galangin was poorly metabolized in untreated Caco-2 cells, whereas 30% of the galangin was oxidized to kaempferol in Caco-2 cells pretreated with TCDD (**Figure 7A**). ANF suppressed the CYP1A1-mediated oxidation of galangin to kaempferol in a dose-dependent manner. Furthermore, the two galangin glucuronoconjugates (t_R of 10.9 and 11.7 min) produced by TCDD-pretreated Caco-2 cells were reduced 0.74- and 0.67-fold, respectively, from that by untreated Caco-2 cells, and these reductions were recovered to the untreated condition by ANF treatment (data not shown).

DISCUSSION

Galangin is present in high concentrations in medicinal plants and a product derived from beehives. Because results from in vitro and in vivo studies indicated that galangin with antioxidative and free radical scavenging activities is capable of modulating enzyme activities and suppressing the genotoxicity of chemicals, it may be a promising candidate for cancer chemoprevention (*12*). Furthermore, galangin suppressed AhR activation and prevented PAH-induced inhibition of cell growth and pre-B cell apoptosis (*13*, *14*). The present study clearly indicates, for the first time, that dioxins change the metabolism and functions of food factors such as galangin by altering the metabolic enzyme activity in intestinal epithelial cells. Here we have shown that galangin, after permeating TCDD-pretreated Caco-2 cell monolayers, reduced its antagonistic activity toward CYP1A1 expression. The oxidative metabolism of galangin to kaempferol by TCDD-induced CYP1A1 in Caco-2 cells is also demonstrated. Our previous study focusing on the search for flavonoids that attenuated TCDD toxicity showed that galangin significantly inhibited TCDD-induced CYP1A1 transcriptional activity by >90%, whereas kaempferol had a much weaker inhibitory effect (*5*). We therefore considered that the reduced inhibitory activity of galangin after it permeated

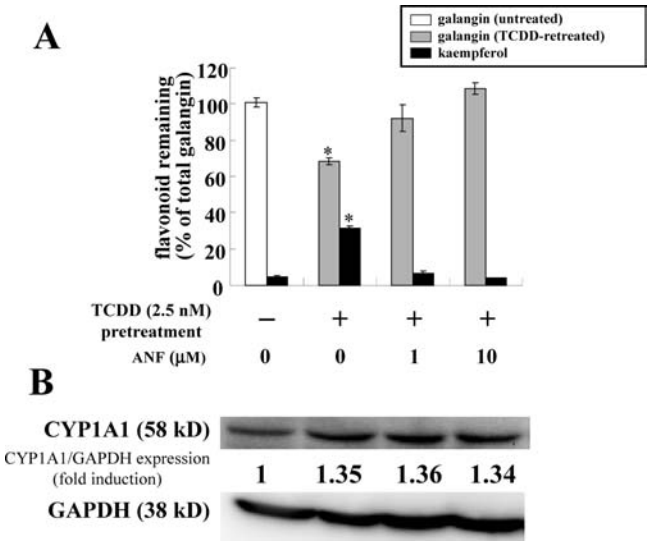

Figure 7. Effect of ANF on the oxidation of galangin to kaempferol by Caco-2 cells pretreated with TCDD. TCDD-pretreated or untreated Caco-2 cells were incubated with 10 μM galangin and ANF for 3 h. (**A**) Galangin and kaempferol were detected by LC-MS/MS. Data are expressed as a percentage of the total amount of galangin used and are presented as the mean ± SE ($n = 3$). *, $p < 0.05$, significantly different from the values for the untreated group analyzed by Tukey's multiple-comparison test. (**B**) The expression of CYP1A1 protein in these cells was analyzed by Western blotting. Relative protein expression (control is set as 1) normalized to GAPDH represents two independent experiments.

TCDD-pretreated Caco-2 cells resulted from the oxidative metabolism of galangin to kaempferol.

Otake and Walle (*15*) demonstrated that galangin was oxidized to kaempferol by human liver microsomes and recombinant enzymes such as CYP1A1, CYP1A2, and CYP2C9 but not CYP3A4. Human intestinal epithelial Caco-2 cells have a different pattern of CYPs compared to hepatocytes. Caco-2 cells express CYP1A1, CYP2E1, and CYP3A but not CYP1A2 and CYP2C9/10 (*16*). CYP1A1 was specifically induced in Caco-2 cells by AhR ligands, whereas CYP1A2 was not (*8*). These observations support our conclusion that the oxidative metabolism of galangin in Caco-2 cells was mainly catalyzed by CYP1A1.

About 30% of galangin was metabolized in TCDD-treated Caco-2 cells in 3 h, being converted to kaempferol (**Figure 7**). Meanwhile, the experimental results using recombinant human CYP1A1 indicated that galangin was totally metabolized and disappeared after 45 min of incubation (**Figure 6**). Only 40% of galangin was detectable as the oxidative metabolite kaempferol; other metabolites were not detected by LC-MS/MS analysis. In the absence of conjugation enzymes such as UGTs and efflux transporters, galangin and kaempferol would be readily metabolized by CYP1A1 and converted to other types of metabolites, although they were not detectable in the analytical system used in the present study. The complicated topology of metabolic enzymes in Caco-2 cells may also be the cause for the different metabolic pattern of galangin (**Figure 7**) compared to that in a recombinant CYP1A1 solution (**Figure 6**).

We demonstrated two glucuronidates of galangin and the expression of UGT1A in Caco-2 cells. Galangin was metabolized by human hepatocytes to two major glucuronides conjugated at the 7- and 3-positions, the reactions being catalyzed mainly by the UGT1A9 isoform in addition to the UGT1A1 and UGT2B15 isosforms (*17*). In the case of other flavonoids, quercetin (3,5,7,3′,4′-pentahydroxyflavone), UGT1A9 (in human liver), and UGT1A1/UGT1A8 (in intestines) are involved in glucuronidation, the formation rate of 3-*O*-glucuronidate in the human intestines (in contrast to human liver) being more than that of 7-*O*-glucuronidate (*18*). It has also been reported that because of strong hydrogen bonding of the 5-OH hydrogen with the 4-keto, conjugation at the 5-OH position does not readily occur (*19*). Taken together, the two glucuronidates of galangin obtained in the present study were probably conjugated through the 7- or 3-hydroxyl group, although the rate of glucuronidation with the participation of UGTs seems to be different from the result in the previous study with hepatocytes (*17*).

Otake et al. (*17*) also indicated that galangin primarily underwent glucuronidation and sulfation with only a small degree of oxidation, corresponding to the results in the present study. Meanwhile, CYP1A1 overexpressed by TCDD treatment inhibited the glucuronidation of galangin by UGT, whereby the oxidation to kaempferol was dominant over the glucuronidation after 3 h of incubation (**Figure 7**). This observation is attributed to the differing topologies between CYP and UGT. An entire molecule containing the functional domain of CYP, which is anchored by the N-terminal region to the endoplasmic reticulum (ER), is present in the cytosol (*20*). In clear contrast to CYP, UGT is anchored to the ER membrane by the transmembrane domain near the C-terminus, and the main body of the enzyme (including the catalytic site) is believed to be present in the ER lumen (*21*). This mode of topology causes latency, a diagnostic feature of UGT. On the other hand, it has been assumed that CYP associates with UGT and functions not only as a producer but also as a transporter of the substrate needed by UGT (*22*). We therefore predicted that overexpressed CYP1A1 would metabolize galangin in the cytosol more rapidly than UGT and facilitate the glucuronidation of kaempferol by UGT because of transport of the substrate in the ER lumen.

The Caco-2 cell monolayer model expresses efflux transporters such as multidrug resistance 1 (MDRl) (*23*), multidrug resistance-associated proteins (MRPs) (*24*), and breast cancer resistance protein (BCRP) (*25*) as well as a series of metabolizing enzymes (*6*). Therefore, it is commonly used for investigating the absorption mechanism for dietary substances and drugs. In particular, MRP2 and MRP3, which have been found on the apical and basal sides of the intestinal epithelium, are responsible for excretion of conjugated metabolites to the lumen and blood supply, respectively (*26*). Studies using apigenin and chrysin have shown that these flavonoids were extensively metabolized in Caco-2 cells and that their glucuronide and sulfate conjugates were excreted to the apical side by MRP and organic anion transporters (*27*, *28*). The selective localization of galangin glucuronide (t_R of 11.7) in the present study suggests that an active transporter must also be involved. The absence of galangin glucuronide on the basal side may imply that this compound is a very good substrate for transporters on the apical side (e.g., MRP2) but a poor substrate for transporters on the basal side (e.g., MRP3).

The intestinal tract could be exposed to a high concentration of dioxins. TCDD has been reported to reduce intestinal cholecystokinin (*29*), retinoids (*30*, *31*), and Ca^{2+} transportation (*32*). Information concerning the effects of dioxins on intestinal absorption and metabolism is limited. Ishida et al. (*33*) reported that a single oral administration of TCDD to C57BL/6J mice produced changes to the villous structure and nuclear/cytoplasm ratio in the intestinal epithelial cells. The expression of the intestinal sodium−glucose cotransporter 1 and level of serum glucose were also increased by TCDD administration. Treatment of Caco-2 cells with the AhR agonist indol-3-carbinol induced the expression of CYP1A1, CYP1B1, and BCRP. Consequently, these inducible enzymes enhanced the metabolism of the procarcinogen

benzo[*a*]pyrene (BP) followed by increased transport of the resultant carcinogens to the apical compartment (*34*, *35*). These studies support our hypothesis that an AhR agonist such as TCDD would change the expression of metabolizing enzymes and transporters, thereby modulating the detoxification process in the intestine.

In summary, our results indicate that TCDD-induced CYP1A1 converted AhR-antagonistic galangin to less antagonistic kaempferol in Caco-2 cells. This provides strong evidence that TCDD affected the metabolism of intestinal cells and altered the biological functions of food factors during intestinal absorption.

ABBREVIATIONS USED

AhR, aryl hydrocarbon receptor; ANF, α-naphthoflavone; BCRP, breast cancer resistance protein; CYP, cytochrome P450; DMEM, Dulbecco's modified Eagle's medium; DMSO, dimethyl sulfoxide; ER, endoplasmic reticulum; PVDF, polyvinylidene difluoride; IgG-HRP, immunoglobulin G−horseradish peroxidase; MRM, multiple reaction monitoring; MRPs, multidrug resistance-associated proteins; TCDD, 2,3,7,8-tetrachlorodibenzo-*p*-dioxin; UGT, UDP-glucuronosyltransferase.

LITERATURE CITED

(1) Mimura, J.; Fujii-Kuriyama, Y. Functional role of AhR in the expression of toxic effects by TCDD. *Biochim. Biophys. Acta* **2003**, *1619* (3), 263–268.

(2) Liem, A. K.; Furst, P.; Rappe, C. Exposure of populations to dioxins and related compounds. *Food Addit. Contam.* **2000**, *17* (4), 241–259.

(3) Travis, C. C.; Hattemer-Frey, H. A. Human exposure to dioxin. *Sci. Total Environ.* **1991**, *104* (1−2), 97–127.

(4) Tutel'yan, V. A.; Gapparov, M. M.; Telegin, L. Y.; Devichenskii, V. M.; Pevnitskii, L. A. Flavonoids and resveratrol as regulators of Ah-receptor activity: protection from dioxin toxicity. *Bull. Exp. Biol. Med.* **2003**, *136* (6), 533–539.

(5) Hamada, M.; Satsu, H.; Natsume, Y.; Nishiumi, S.; Fukuda, I.; Ashida, H.; Shimizu, M. TCDD-induced CYP1A1 expression, an index of dioxin toxicity, is suppressed by flavonoids permeating the human intestinal Caco-2 cell monolayers. *J. Agric. Food Chem.* **2006**, *54* (23), 8891–8898.

(6) Sun, D.; Lennernas, H.; Welage, L. S.; Barnett, J. L.; Landowski, C. P.; Foster, D.; Fleisher, D.; Lee, K. D.; Amidon, G. L. Comparison of human duodenum and Caco-2 gene expression profiles for 12,000 gene sequences tags and correlation with permeability of 26 drugs. *Pharm. Res.* **2002**, *19* (10), 1400–1416.

(7) Galijatovic, A.; Otake, Y.; Walle, U. K.; Walle, T. Extensive metabolism of the flavonoid chrysin by human Caco-2 and Hep G2 cells. *Xenobiotica* **1999**, *29* (12), 1241–1256.

(8) Boulenc, X.; Bourrie, M.; Fabre, I.; Roque, C.; Joyeux, H.; Berger, Y.; Fabre, G. Regulation of cytochrome P450IA1 gene expression in a human intestinal cell line, Caco-2. *J. Pharmacol. Exp. Ther.* **1992**, *263* (3), 1471–1478.

(9) Munzel, P. A.; Schmohl, S.; Heel, H.; Kalberer, K.; Bock-Hennig, B. S.; Bock, K. W. Induction of human UDP glucuronosyltransferases (UGT1A6, UGT1A9, and UGT2B7) by *t*-butylhydroquinone and 2,3,7,8-tetrachlorodibenzo-*p*-dioxin in Caco-2 cells. *Drug Metab. Dispos.* **1999**, *27* (5), 569–573.

(10) Natsume, Y.; Satsu, H.; Kitamura, K.; Okamoto, N.; Shimizu, M. Assessment system for dioxin absorption in the small intestine and prevention of its absorption by food factors. *Biofactors* **2004**, *21* (1−4), 375–377.

(11) Wilhelmsson, A.; Whitelaw, M. L.; Gustafsson, J. A.; Poellinger, L. Agonistic and antagonistic effects of α-naphthoflavone on dioxin receptor function. Role of the basic region helix−loop−helix dioxin receptor partner factor Arnt. *J. Biol. Chem.* **1994**, *269* (29), 19028–19033.

(12) Heo, M. Y.; Sohn, S. J.; Au, W. W. Anti-genotoxicity of galangin as a cancer chemopreventive agent candidate. *Mutat. Res.* **2001**, *488* (2), 135–150.

(13) Ciolino, H. P.; Yeh, G. C. The flavonoid galangin is an inhibitor of CYP1A1 activity and an agonist/antagonist of the aryl hydrocarbon receptor. *Br. J. Cancer* **1999**, *79* (9−10), 1340–1346.

(14) Quadri, S. A.; Qadri, A. N.; Hahn, M. E.; Mann, K. K.; Sherr, D. H. The bioflavonoid galangin blocks aryl hydrocarbon receptor activation and polycyclic aromatic hydrocarbon-induced pre-B cell apoptosis. *Mol. Pharmacol.* **2000**, *58* (3), 515–525.

(15) Otake, Y.; Walle, T. Oxidation of the flavonoids galangin and kaempferide by human liver microsomes and CYP1A1, CYP1A2, and CYP2C9. *Drug Metab. Dispos.* **2002**, *30* (2), 103–105.

(16) Lampen, A.; Bader, A.; Bestmann, T.; Winkler, M.; Witte, L.; Borlak, J. T. Catalytic activities, protein- and mRNA-expression of cytochrome P450 isoenzymes in intestinal cell lines. *Xenobiotica* **1998**, *28* (5), 429–441.

(17) Otake, Y.; Hsieh, F.; Walle, T. Glucuronidation versus oxidation of the flavonoid galangin by human liver microsomes and hepatocytes. *Drug Metab. Dispos.* **2002**, *30* (5), 576–581.

(18) Boersma, M. G.; van der Woude, H.; Bogaards, J.; Boeren, S.; Vervoort, J.; Cnubben, N. H.; van Iersel, M. L.; van Bladeren, P. J.; Rietjens, I. M. Regioselectivity of phase II metabolism of luteolin and quercetin by UDP-glucuronosyl transferases. *Chem. Res. Toxicol.* **2002**, *15* (5), 662–670.

(19) Boutin, J. A.; Meunier, F.; Lambert, P. H.; Hennig, P.; Bertin, D.; Serkiz, B.; Volland, J. P. In vivo and in vitro glucuronidation of the flavonoid diosmetin in rats. *Drug Metab. Dispos.* **1993**, *21* (6), 1157–1166.

(20) Shimozawa, O.; Sakaguchi, M.; Ogawa, H.; Harada, N.; Mihara, K.; Omura, T. Core glycosylation of cytochrome P-450(arom). Evidence for localization of N terminus of microsomal cytochrome P-450 in the lumen. *J. Biol. Chem.* **1993**, *268* (28), 21399–21402.

(21) Meech, R.; Mackenzie, P. I. Structure and function of uridine diphosphate glucuronosyltransferases. *Clin. Exp. Pharmacol. Physiol.* **1997**, *24* (12), 907–915.

(22) Taura, K.; Naito, E.; Ishii, Y.; Mori, M. A.; Oguri, K.; Yamada, H. Cytochrome P450 1A1 (CYP1A1) inhibitor alpha-naphthoflavone interferes with UDP-glucuronosyltransferase (UGT) activity in intact but not in permeabilized hepatic microsomes from 3-methylcholanthrene-treated rats: possible involvement of UGT-P450 interactions. *Biol. Pharm. Bull.* **2004**, *27* (1), 56–60.

(23) Hunter, J.; Jepson, M. A.; Tsuruo, T.; Simmons, N. L.; Hirst, B. H. Functional expression of P-glycoprotein in apical membranes of human intestinal Caco-2 cells. Kinetics of vinblastine secretion and interaction with modulators. *J. Biol. Chem.* **1993**, *268* (20), 14991–14997.

(24) Hirohashi, T.; Suzuki, H.; Chu, X. Y.; Tamai, I.; Tsuji, A.; Sugiyama, Y. Function and expression of multidrug resistance-associated protein family in human colon adenocarcinoma cells (Caco-2). *J. Pharmacol. Exp. Ther.* **2000**, *292* (1), 265–270.

(25) Gutmann, H.; Hruz, P.; Zimmermann, C.; Beglinger, C.; Drewe, J. Distribution of breast cancer resistance protein (BCRP/ABCG2) mRNA expression along the human GI tract. *Biochem. Pharmacol.* **2005**, *70* (5), 695–699.

(26) Borst, P.; Evers, R.; Kool, M.; Wijnholds, J. The multidrug resistance protein family. *Biochim. Biophys. Acta* **1999**, *1461* (2), 347–357.

(27) Hu, M.; Chen, J.; Lin, H. Metabolism of flavonoids via enteric recycling: mechanistic studies of disposition of apigenin in the Caco-2 cell culture model. *J. Pharmacol. Exp. Ther.* **2003**, *307* (1), 314–321.

(28) Walle, U. K.; Galijatovic, A.; Walle, T. Transport of the flavonoid chrysin and its conjugated metabolites by the human intestinal cell line Caco-2. *Biochem. Pharmacol.* **1999**, *58* (3), 431–438.

(29) Lee, H. M.; He, Q.; Englander, E. W.; Greeley, G. H., Jr. Endocrine disruptive effects of polychlorinated aromatic hydrocarbons on intestinal cholecystokinin in rats. *Endocrinology* **2000**, *141* (8), 2938–2944.

(30) Brouwer, A.; Hakansson, H.; Kukler, A.; Van den Berg, K. J.; Ahlborg, U. G. Marked alterations in retinoid homeostasis of Sprague−Dawley rats induced by a single i.p. dose of 10 micrograms/kg of 2,3,7,8-tetrachlorodibenzo-*p*-dioxin. *Toxicology* **1989**, *58* (3), 267–283.

(31) Hanberg, A.; Nilsson, C. B.; Trossvik, C.; Hakansson, H. Effect of 2,3,7,8-tetrachlorodibenzo-*p*-dioxin on the lymphatic absorption of a single oral dose of [^{3}H]retinol and on the intestinal retinol esterification in the rat. *J. Toxicol. Environ. Health A* **1998**, *55* (5), 331–344.

(32) Manis, J.; Kim, G. Stimulation of iron absorption by polychlorinated aromatic hydrocarbons. *Am. J. Physiol.* **1979**, *236* (6), E763–E768.

(33) Ishida, T.; Kan-o, S.; Mutoh, J.; Takeda, S.; Ishii, Y.; Hashiguchi, I.; Akamine, A.; Yamada, H. 2,3,7,8-Tetrachlorodibenzo-*p*-dioxin-induced change in intestinal function and pathology: evidence for the involvement of arylhydrocarbon receptor-mediated alteration of glucose transportation. *Toxicol. Appl. Pharmacol.* **2005**, *205* (1), 89–97.

(34) Ebert, B.; Seidel, A.; Lampen, A. Identification of BCRP as transporter of benzo[*a*]pyrene conjugates metabolically formed in Caco-2 cells and its induction by Ah-receptor agonists. *Carcinogenesis* **2005**, *26* (10), 1754–1763.

(35) Ebert, B.; Seidel, A.; Lampen, A. Induction of phase-1 metabolizing enzymes by oltipraz, flavone and indole-3-carbinol enhance the formation and transport of benzo[a]pyrene sulfate conjugates in intestinal Caco-2 cells. *Toxicol. Lett.* **2005**, *158* (2), 140–151.

Received for review February 25, 2010. Revised manuscript received May 30, 2010. Accepted June 3, 2010. M.H. received a research fellowship for Young Scientists from the Japan Society for the Promotion of Sciences (JSPS). This work was partially supported by a Grant-in Aid for Scientific Research on the Priority Area "Transportsome" and a Grant-in Aid for Scientific Research (S-15108002).